Available online at www.sciencedirect.com

jmr&t Journal of Materials Research and Technology

www.jmrt.com.br

Original Article

# Octylsilanol and Ce(III) ions – alternative corrosion inhibitors for carbon steel in chloride neutral solutions

*Fernando Cotting*[a,*], *Idalina Vieira Aoki*[b]

[a] *Chemical Engineering Department, Federal University of Minas Gerais (UFMG), Av. Antonio Carlos, 6627, ZIP 31270-901, Belo Horizonte, MG, Brazil*

[b] *Chemical Engineering Department of Polytechnic School of the University of São Paulo, Av. Prof. Luciano Gualberto, Trav. 3, Nr. 380 CEP, 05508-010, São Paulo, Brazil*

ARTICLE INFO

*Article history:*
Received 2 February 2020
Accepted 3 June 2020
Available online 18 June 2020

*Keywords:*
Carbon steel
Cerium salt
Chloride solution
EIS
Octylsilanol
SVET

ABSTRACT

This work evaluated a corrosion inhibitor that consists of a mixture of a long chain silanol and cerium(III) salt, to protect carbon steel in 0.1 mol $L^{-1}$ NaCl solution. The inhibitor solution was obtained after hydrolysis of the silane in the presence of the cerium salt. The silane concentration was kept constant at 400 ppm, while the cerium ions variated in 25, 50, and 100 ppm. The electrochemical measurements showed inhibition efficiency (% I.E.) above 96% for carbon steel in NaCl 0.1 mol $L^{-1}$, in the best condition of the mixture of silanol and Ce (III) ions. The Raman spectroscopy confirmed the presence of inhibitors in the carbon steel surface even out of the solution containing the inhibitors as a persistent adsorbed film. Contact angle measurements showed the surface hydrophobicity imparted by the adsorbed corrosion inhibitor layer. SVET measurements confirmed that the corrosion inhibitors mixture can block both anodic and cathodic reactions. The studied inhibitors showed to be more efficient and/or cheaper than traditional corrosion inhibitors for neutral media.



## 1. Introduction

The corrosion on metals can be mitigated with corrosion inhibitors. Corrosion inhibitors can adsorb on the metallic surface and blocking the anodic reactions, minimizing the reduction of the oxidant species or blocking the cathodic reactions. Usually, the inhibitor excess in the electrolyte accelerates the metal dissolution, due to their irregular and disordered adsorption on the metallic surface [1–4]. There are many papers in which corrosion inhibitors have been evaluated in acidic media [5–8]. Nevertheless, there is a deficiency in studies with corrosion inhibitors for neutral media, which is very important, once this electrolyte represents most environments away from the sea.

The studies for more effective corrosion inhibitors – in the past decades – led to the development of more complex substances, which are very harmful, for example chromium compounds and arsenic salts. Therefore, new less harmful and green corrosion inhibitors have been developed [1,2]. The green chemistry, using corrosion inhibitors extracted from vegetables, is a good strategy to keep away from harm-

* *Corresponding author.*
E-mail: fernando@deq.ufmg.br (F. Cotting).

https://doi.org/10.1016/j.jmrt.2020.06.011

ful substances; nevertheless, this route can be limited, once the vegetables are consumed in humans' diet. In this direction, silanes are substances of low toxicity [9], which after suffering hydrolysis reaction incorporate in their chain OH groups, resulting in the so-called silanols. When a substrate has hydroxyls groups on its surface, the silanol is capable of adsorbing on this substrate by interacting by hydrogen bonds with these –OH groups creating a protective adsorbed barrier layer against corrosion and subsequent formation of siloxane bonds during the curing process of the final film [9–20], when it is the case of pre-treatments. There are few studies using silanes as corrosion inhibitors [21] since the vast majority of studies employ silanes as a pretreatment to form thin films on a metallic surface.

The rare earth salts (RES), especially of lanthanum and cerium, are also an alternative against corrosion for metallic surfaces, like silanes, they present low toxicity and a good performance in inhibiting corrosion of different metals, mainly in neutral solutions [22–28]. These salts show good efficiency when their metallic ions are used alone and above the concentration of 250 ppm [27,28], which can render the use of these salts very expensive.

In neutral solutions, the metal's corrosion is controlled by the oxygen reduction Eq. (1) leading to the formation of hydroxyl ions. In the presence of hydroxyls, the released metallic ions or added RES precipitate in the form of hydroxides Eq. (2) on the cathodic sites, blocking the advance of the cathodic reactions [24].

$$O_2 + 2H_2O + 4e \rightarrow 4OH- \quad (1)$$

$$Ce^{3+} + 3OH- \rightarrow Ce(OH)_3 \quad (2)$$

The doping of silanes with RES – in the thin films formation – imparts to different types of substrates good corrosion protection, as stated by different research groups [2,3,9,29] owing to a kind of synergism.

This work aims to evaluate the performance of a long chain silanol (octyltriethoxysilanol) doped with Ce (III) chloride as corrosion inhibitors for 1020 carbon steel in 0.1 mol $L^{-1}$ NaCl by electrochemical techniques, contact angle measurements and Raman spectroscopy.

## 2. Experimental

All reagents were used as received. Octyltriethoxysilane – Silquest A137 silane – was donated by Momentive Performance. Cerium (III) chloride heptahydrate – $CeCl_3{\cdot}7H_2O$ was purchased from Vetec.

Carbon steel samples of 3 cm × 4 cm × 0.1 cm dimensions were ground with 320, 400 and 600 emery papers, in this sequence, de-greased in an acetone ultrasonic bath for 5 min and immersed in a 2.5% NaOH solution for 10 min to activate the formation of hydroxyl groups in the metallic surface. After alkaline treatment, the samples were washed in distilled water and dried in a hot air stream.

### 2.1. Hydrolysis of the silane

In a solvent solution ethanol/water 50/50% (v/v), acidified to pH 5.0 with acetic acid, were added different concentrations of the Ce (III) ions from $CeCl_3{\cdot}7H_2O$. This solution ethanol/water with pH adjusted and containing cerium salt was submitted to sonification for 5 min. This procedure induces the formation of radicals such as OH [19] that can promote addiction polymerization reactions reticulating the adsorbed molecules what makes the layer more protective. Then, 4% (w/w) of octyltriethoxysilane was added. This solution was stirred for 24 h at room temperature to allow for hydrolysis.

For EIS measurements and polarization curves, the electrolyte used was 0.1 mol $L^{-1}$ NaCl solution. In this solution 400 ppm octylsilanol was added containing different concentrations of Ce (III) ions.

The neutral saline solution was employed due to the fact that in chemical process plants, their devices are frequently exposed to this electrolyte such as heat exchangers, cooling towers systems, and oil and gas production and refinery units.

The SVET measurements were performed in 0.01 mol $L^{-1}$ NaCl solution in order to not provoke an intense corrosion process making possible to follow the action of the added inhibitors.

### 2.2. Electrochemical measurements

A three-electrode electrochemical cell was used, consisting of the working electrode (WE) with 1.0 $cm^2$ of the exposed area, Ag/AgCl/KCl(sat.) electrode as reference (RE) and a platinum foil as a counter electrode (CE). The electrochemical tests were performed after 3 h of immersion in the electrolyte solution till a stationary open circuit potential, $E_{oc}$ was achieved.

Electrochemical impedance spectroscopy (EIS) measurements were performed at room temperature in a Faraday cage. The measuring frequency ranged from 50 kHz down to 5 mHz. The voltage disturbance around the open circuit potential was 10 mV r.m.s.

In linear polarization resistance measurements, the WE has polarized in the range ±20 mV versus $E_{oc}$ at a scan rate of 0.167 mV $s^{-1}$. The potentiodynamic polarization curves were obtained in the range from –250 to +250 mV versus $E_{oc}$ at a scan rate of 0.5 mV $s^{-1}$.

The scanning vibrating electrode technique (SVET) measurements were performed using an Applicable Electronics apparatus, controlled by the ASET program (Sciencewares). Insulated Pt–Ir probes (Microprobe, Inc.) with black platinum deposited on a spherical tip of 10 μm diameter were used as a vibrating electrode (probe) for the SVET system. The probe was placed 100 μm above the surface. The only vertical component of the current was used.

### 2.3. Contact angle measurements

The contact angle measurements were performed in the Dataphysics OCA20 device, coupled to the SCA20 software. The method used was the water sessile drop method.

**Table 1 – $E_{corr}$ values obtained for carbon steel after 3 h of immersion in NaCl 0.1 mol $L^{-1}$ containing 400 ppm of pure octylsilanol and with different Ce (III) ions concentrations.**

| Inhibitors concentration | Ecorr (mV/Ag/AgCl/$KCl_{sat}$) |
|---|---|
| Blank (without inhibitor) | −672 ± 22 |
| 400 ppm octylsilanol | −514 ± 8 |
| 400 ppm octylsilanol + 25 ppm Ce (III) | −489 ± 12 |
| 400 ppm octylsilanol + 50 ppm Ce (III) | −470 ± 10 |
| 400 ppm octylsilanol + 100 ppm Ce (III) | −526 ± 25 |

### 2.4. *Raman spectroscopy*

The Raman spectroscopy results were obtained with a confocal Raman spectrophotometer Horiba Jobin Yvon, model Labram HR. The assays were carried in the wavenumber range from 100 $cm^{-1}$ to 1200 $cm^{-1}$, at room temperature on previously immersed for 24 h carbon steel samples on the 0.1 mol $L^{-1}$ NaCl with 400 ppm of octylsilanol + 50 ppm of Ce(III) ions and subsequently withdrawn from the inhibited aggressive solution, washed with water and dried in a hot air stream. So, Raman spectra were obtained on the remaining adsorbed film still present on carbon steel samples. The analyses were performed at the Corrosion and Protection Laboratory, University of Antioquia, Medellin, Colombia.

All experiments were conducted in triplicate.

## 3. Results and discussion

### 3.1. *Corrosion potential*

Table 1 shows the $E_{oc}$ values for carbon steel that coincide with corrosion potential, $E_{corr}$, for different conditions, after 3 h of immersion. The presence of Ce (III) ions, as well as the octylsilanol, shifted the $E_{corr}$ to more positive values, indicating that the corrosion inhibitor has a pronounced action as an anodic inhibitor.

### 3.2. *Linear polarization resistance (Rp) measurements*

The Rp values are shown in Table 2. The corrosion inhibition efficiency (% I.E.) was determined as noted in Eq. (3):

$$\%\text{I.E.} = \frac{Rp_{inib} - Rp_{blank}}{Rp_{inib}} \times 100 \quad (3)$$

where the $Rp_{inhib}$ and $Rp_{blank}$ are the polarization resistance for inhibited and uninhibited aggressive medium, respectively, determined by Stern & Geary method.

**Table 3 – Price, toxicity and degradability of some corrosion inhibitors for neutral solutions.**

| Compound | Price (USD/kg) | Toxicity | Degradability |
|---|---|---|---|
| 2-Mercaptobenzimidazole | 228.00 | Very high | Poor |
| Cerium (III) chloride | 818.00 | Low | Fair |
| Zinc chromate | 6,600.00 | Very high | Poor |
| Sodium benzoate | 41.0 | Low | Excellent |
| Sodium molybdate | 513.00 | Moderate | Fair |
| Octyltriethoxysilane | 100.00 | Low | Fair |
| Zinc chloride | 100.00 | High | Poor |

The hydrolyzed octylsilane molecule without the addition of Ce (III) ions did not offer good corrosion inhibition for carbon steel. Nonetheless, in the presence of Ce (III) ions the % I.E. was far higher effective. This improved performance occurs due to the pH decrease in the cerium chloride presence during the hydrolysis, which is more pronounced for higher Ce (III) concentrations. Therefore, for lower Ce (III) concentration, about 50 ppm, the precipitation of cerium hydroxides is also assisted. The results obtained show that the addition of Ce (III) ions at different concentrations – along with 400 ppm octylsilanol – provides corrosion protection for carbon steel. The Rp increases with the increase of Ce (III) concentration until reaching 50 ppm, where a maximum value of 97.8 % I.E. is reached. However, at 100 ppm addition, the inhibiting efficiency decreases to 88.1%. These results reveal an excellent synergism between the two corrosion inhibitors, because the corrosion rate for carbon steel, in chloride neutral solutions only with Ce (III) ions, decrease in concentrations higher than 200 ppm [24]. Nevertheless, when these ions are in combination with 400 ppm of octylsilanol, 50 ppm of Ce (III) ions are enough.

Table 3 shows the price, toxicity, and degradability for some of the traditional corrosion inhibitors – for neutral saline solutions – and for the studied compounds in this study. The presented information was obtained from Safety Data Sheets (SDS) and from the main chemicals sellers.

From Table 3 it is clear to verify that the studied compounds present advantages when compared with traditional corrosion inhibitors. The main advantage is in their low toxicity, once that majority of those reputable inhibitors substances are very harmful. Besides, when compared with the inhibitors presented in Table 3, the low cost of the studied compounds is very encouraging, because it enables the use of these substances on an industrial scale/practice.

Table 4 presents the usual concentration and the obtained inhibition efficiency by these well-known corrosion inhibitors for carbon steel in neutral solutions. Comparing these values

**Table 2 – Values of $E_{corr}$, Rp, coverage degree ($\theta$) and % I.E. obtained for carbon steel in NaCl 0.1 mol $L^{-1}$ containing 400 ppm octylsilanol and different Ce (III) ions concentrations.**

| Inhibitors concentration (ppm) | $E_{corr}$ (mV/Ag/AgCl/$KCl_{sat}$) | Rp (kΩ $cm^2$) | Coverage degree, $\theta$ | %I.E. |
|---|---|---|---|---|
| Blank (without inhibitor) | −672 | 1.7 ± 0.8 | – | – |
| 400 ppm octylsilanol | −514 | 3.2 ± 0.3 | 0.469 | 46.9 |
| 400 ppm octylsilanol+ 25 ppm Ce (III) | −489 | 56.9 ± 2.0 | 0.970 | 97.0 |
| 400 ppm octylsilanol+ 50 ppm Ce (III) | −470 | 77.3 ± 0.9 | 0.978 | 97.8 |
| 400 ppm octylsilanol+ 100 ppm Ce (III) | −526 | 14.3 ± 1.2 | 0.881 | 88.1 |

**Table 4 – Usual concentration and efficiency of well-known corrosion inhibitors for neutral solutions.**

| Compound | Concentration (ppm) | Efficiency (%) | Reference |
|---|---|---|---|
| 2-Mercaptobenzimidazole | 3,000 | 85.3 | [30] |
| Chromate | 572 | 99.0 | [31] |
| Sodium benzoate | 57,600 | 53.2 | [32] |
| Sodium molybdate | 200 | 61.0 | [33] |
| Zinc salt | 200 | 77.0 | [34] |

with Table 2 data, it is evident that the mixture octylsilanol and Ce (III) presented promising results, even when compared with sodium benzoate, because approximately one hundred and twenty times more inhibitor is needed to present a little more than half of the protection offered by the studied compounds in this paper.

### 3.3. *Electrochemical impedance spectroscopy (EIS)*

Analyzing the impedance diagrams shown in Fig. 1 Fig. 1, an increase in the impedance modulus at low frequencies can be observed in the presence of cerium ions, where the concentration of 50 ppm of Ce (III) ions resulted in better performance expressed by higher impedance modulus, confirming the results obtained by Rp measurements. In the Nyquist diagrams, the same behavior can be observed; the presence of cerium ions increases the protection of steel concerning the system that contains only the octylsilanol, increasing the diameter of the capacitive arcs. At Bode diagrams, $\theta \times \log f$, the presence of a new time constant is observed at high frequencies in the presence of cerium ions, resulting in high values of phase angle, indicating the presence of a protective film on the substrate [24–26].

### 3.4. *Potentiodynamic polarization curves*

Polarization curves in Fig. 2 shows that the presence of Ce (III) ions along with 400 ppm of octylsilanol decreased the corrosion rate of carbon steel in NaCl 0.1 mol $L^{-1}$. The lowest corrosion rate was obtained for 50 ppm of Ce (III) ions. These results corroborate the results obtained by other electrochemical techniques. The polarization curves show a large shift in both, anodic and cathodic branches, as a consequence of the adsorption of the octylsilanol molecule and precipitation of cerium hydroxides, respectively.

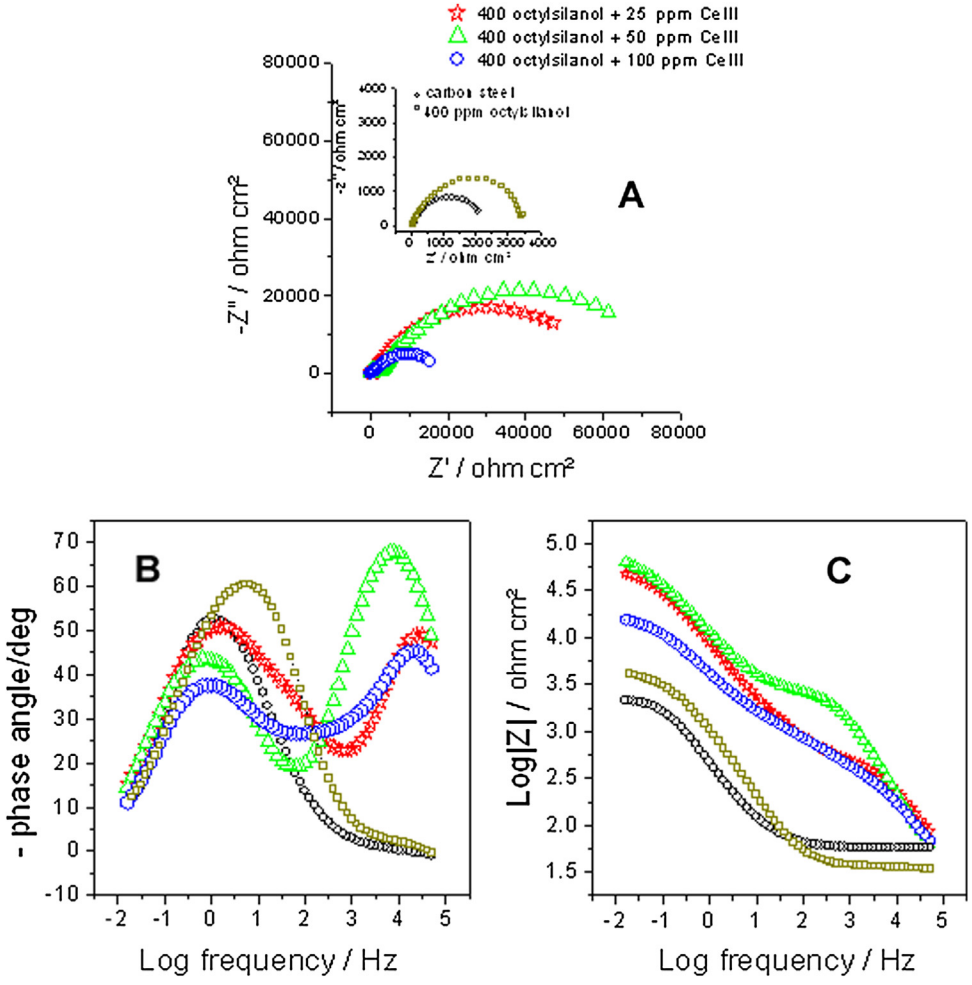


**Fig. 1 – Impedance diagrams. (A) Nyquist, (B) Bode $\theta \times \log f$ and (C) Bode IZI $\times \log f$ for carbon steel after 3 h of immersion in NaCl 0.1 mol $L^{-1}$, with 400 ppm of octylsilanol in the absence and presence of the Ce (III) ions at different concentrations.**

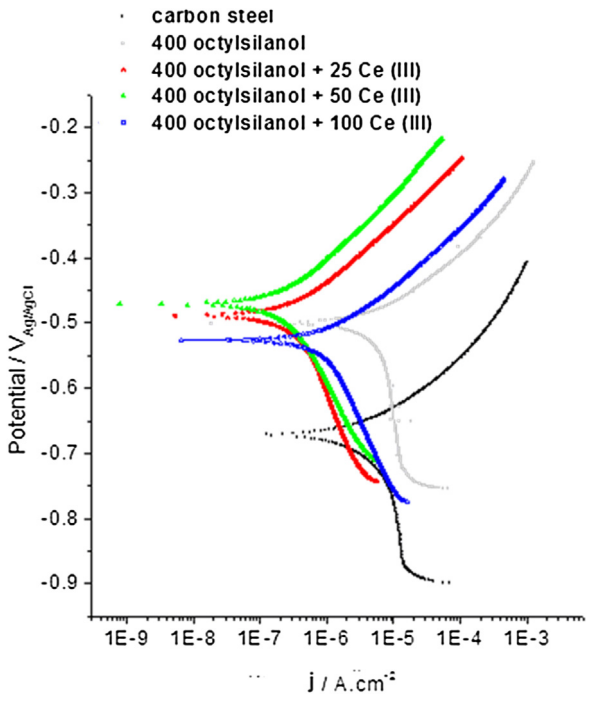


**Fig. 2 – Polarization curves for carbon steel after 3 h of immersion in NaCl 0.1 mol $L^{-1}$, with 400 ppm of octylsilanol in the absence and presence of the Ce (III) ions in different concentrations.**

The corrosion inhibition efficiency (% I.E.) was determined as shown in Eq. (4).

$$\%IE = \frac{icorrblank - icorrinib}{icorrblank} \times 100 \quad (4)$$

where $icorr_{inib}$ and $icorr_{blank}$ are the inhibited and uninhibited condition corrosion current densities, respectively, determined by extrapolation of the cathodic Tafel slope till $E_{oc}$. Corresponding electrochemical parameters are summarized in Table 5. Both anodic and cathodic branches of polarization curves are more polarized in the presence of Ce (III) ions, which allow classifying the inhibitors as mixed-type with a more pronounced anodic behavior.

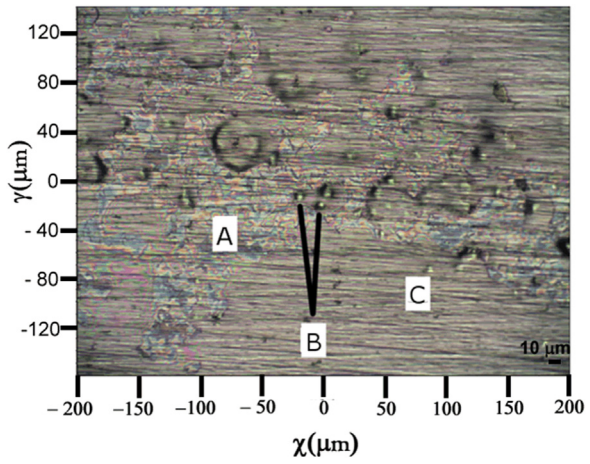


**Fig. 4 – Optical image obtained at the surface of carbon steel coated with corrosion inhibitors, during Raman spectroscopy; (A) region with interference colors; (B) white precipitates region; and (C) a uniform region.**

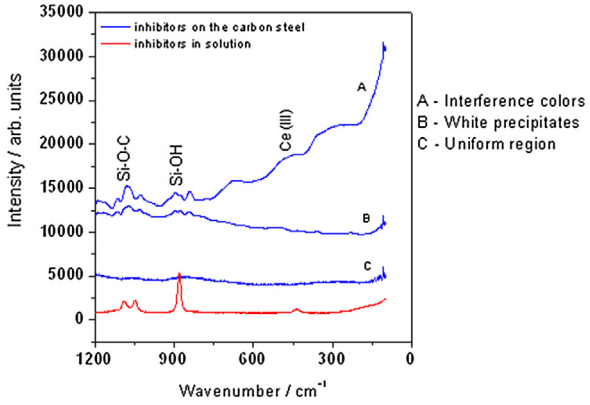


**Fig. 5 – Raman spectra of the corrosion inhibitors on the carbon steel and in solution.**

### 3.5. *Contact angle*

To perform contact angle measurements, carbon steel was immersed for 3 h in NaCl 0.1 mol $L^{-1}$ containing 400 ppm octylsilanol + 50 ppm of Ce (III) ions. The sample was rinsed with

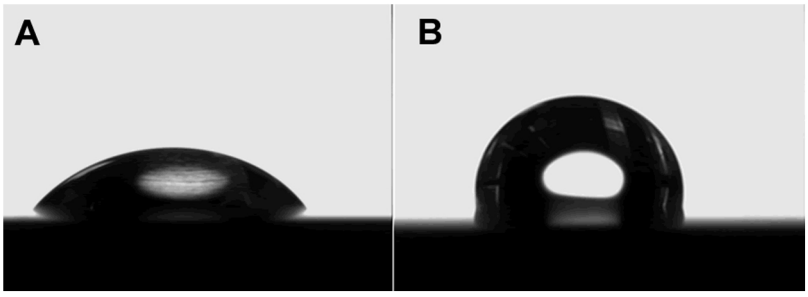


**Fig. 3 – Images obtained during contact angle measurements. (A) Steel with alkaline treatment without inhibitor ($\theta = 58.1° \pm 2.3°$). (B) Steel after 3 h immersion in the aggressive solution containing corrosion inhibitors in the best condition ($\theta = 111.9° \pm 1.1°$).**

**Table 5 – Values of $E_{corr}$, $i_{corr}$, degree of coverage and % I.E. from polarization curves for mild steel in NaCl 0.1 mol $L^{-1}$ containing 400 ppm octylsilanol and different ion concentrations of Ce (III).**

| Inhibitors concentration (ppm) | $E_{corr}$ (mV/Ag/AgCl) | $i_{corr}$ (A/cm$^2$) | Coverage degree, $\theta$ | %I.E. |
|---|---|---|---|---|
| Blank (without inhibitor) | −672 | $2.0 \times 10^{-6} \pm 0.2 \times 10^{-6}$ | – | – |
| 400 ppm octylsilanol | −514 | $2.3 \times 10^{-6} \pm 1.1 \times 10^{-6}$ | 0.13 | 13 |
| 400 ppm octylsilanol+ 25 ppm Ce (III) | −489 | $1.4 \times 10^{-7} \pm 0.7 \times 10^{-7}$ | 0.94 | 94 |
| 400 ppm octylsilanol+ 50 ppm Ce (III) | −470 | $9 \times 10^{-8} \pm 2 \times 10^{-8}$ | 0.96 | 96 |
| 400 ppm octylsilanol+ 100 ppm Ce (III) | −526 | $3.4 \times 10^{-7} \pm 0.3 \times 10^{-7}$ | 0.85 | 85 |

distilled water and dried in a hot air stream. It was observed that the persistent adsorbed film is hydrophobic providing values of contact angle greater than 90º, as shown in Fig. 3.

### 3.6. *Raman spectroscopy*

The Raman spectroscopy analyses were conducted using 400 ppm octylsilanol + 50 ppm Ce (III) ions since it was the best condition previously evaluated. Spectra were obtained for the corrosion inhibitors in solution – after the hydrolysis reaction – and also for corrosion inhibitors adsorbed on carbon steel after immersion for 24 h in the electrolyte, in the presence of inhibitors. The images, obtained and presented in Fig. 4 for carbon steel in the optical microscope associated with the Raman spectrometer, show three different regions: a region with interference colors in Fig. 4A, a white precipitates region in Fig. 4B, and a uniform region in Fig. 4C.

Fig. 5 shows the Raman spectra obtained for the corrosion inhibitors in solution, along with the spectra of the three regions observed on the previously immersed carbon steel in the solution with inhibitors for the best condition. Some peaks are important and characteristic in the analysis of the octylsilanol hydrolysis, such as the peak at 1125–1180 $cm^{-1}$ attributed to the Si—O stretching of Si—O—C bond [19]. In this peak, an increase in the intensity indicates silanol condensation in the adsorbed film [35]. The peak at 840–900 $cm^{-1}$ attributed to Si–OH stretching, indicates the amount of silanol formed during the hydrolysis reaction; thus, an increase in this peak indicates a larger amount of silanol formed, as a consequence of a more effective hydrolysis [36] and finally, the peak in the 400–600 $cm^{-1}$ region, which corresponds to the presence of cerium ions on the sample surface [19,37].

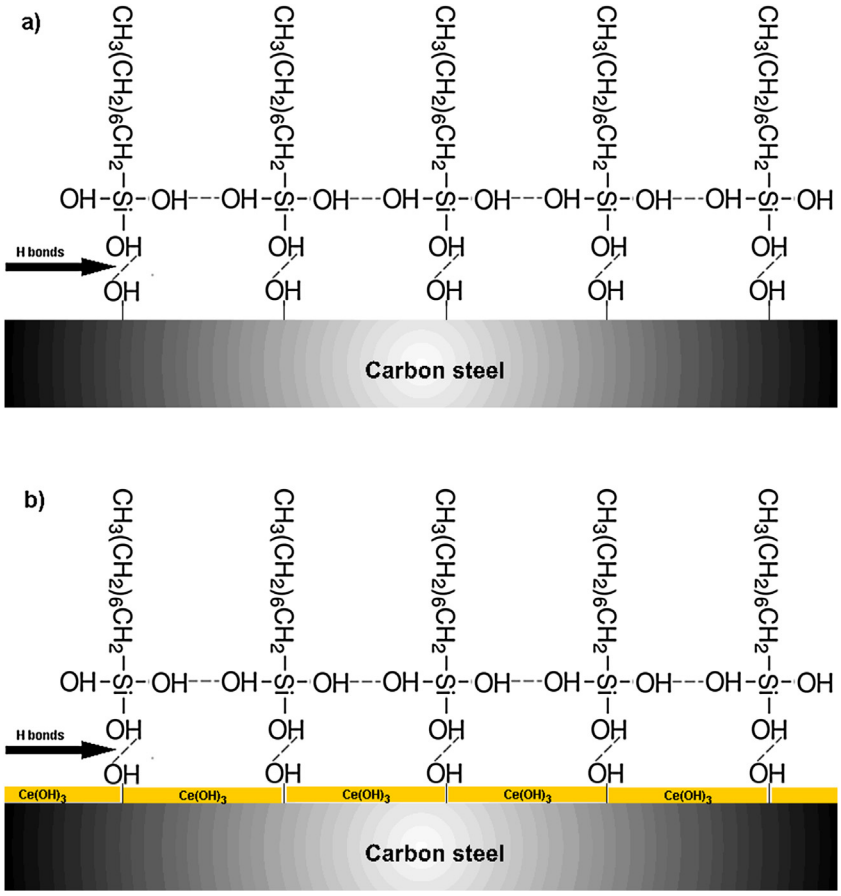


**Fig. 6 – Schematic diagram of the inhibition mechanism: (a) only octylsilanol and (b) 400 ppm of octylsilanol + 50 ppm Ce (III).**

### 3.7. *Comparing the Raman spectra*

The Raman spectra for inhibitors on the steel showed a decrease in the Si—OH stretching vibration at ~877 $cm^{-1}$ compared with inhibitors in solution. This observation is because of the octylsilanol adsorption on the steel [35,36]. The peak at ~1000 $cm^{-1}$ attributed to the condensation of the silanol [35,38] was observed in all conditions, however, for the inhibitors solution this peak is more intense than inhibitors on the steel; this behavior occurs due to the adsorbed layers on steel are very thin, consequently a low intensity in this peak will be observed for this condition.

The band at ~450 $cm^{-1}$ attributed to the presence of Ce (III) ions [19,37], was observed for the inhibitors on the steel – interference colour region – and for the inhibitors in solution. This result shows that the cerium hydroxides did not precipitate uniformly all over the whole surface.

Raman spectroscopy supported the interpretation of obtained electrochemical measurements, confirming that the protection of carbon steel in NaCl 0.1 mol $L^{-1}$ occurs both by the adsorption of silanols and the precipitation of cerium hydroxides on the substrate, hindering the contact of aggressive agents with the carbon steel. The presence of siloxane bonds Si—O—Si indicates a chemical interaction between neighbor silanol molecules on carbon steel.

### 3.8. *Inhibition mechanism of proposed corrosion inhibitors*

When in contact with the electrolyte, the oxidation process of the steel is initiated by the oxygen reduction – Eq. (5) and Eq. (6). The octylsilanol when adsorbed on the substrate, reduce the surface area exposed, as a consequence decreases the steel corrosion rate. However, the adsorbed octylsilanol film is not uniform; hence the corrosive process persists at a considerable speed. Thus, the hydroxyls released during the oxygen reduction leads to local pH increase. At higher pHs – above 9 – and in the potential range between ~−2.2 $V_{EH}$ and +1.4 $V_{EH}$, the thermodynamic stability of the cerium occurs in the form of cerium hydroxide $Ce(OH)_3$ [29]. At $E_{oc}$ values measured in this work, the same is true. Then, the Ce (III) ions present in the electrolyte react with the hydroxyls released in the oxygen reduction Eq. (7) on the cathodic sites, reducing or blocking the cathodic reactions. This effect ensures additional protection afforded by the octylsilanol anodic protection, resulting in a synergism between both corrosion inhibitors.

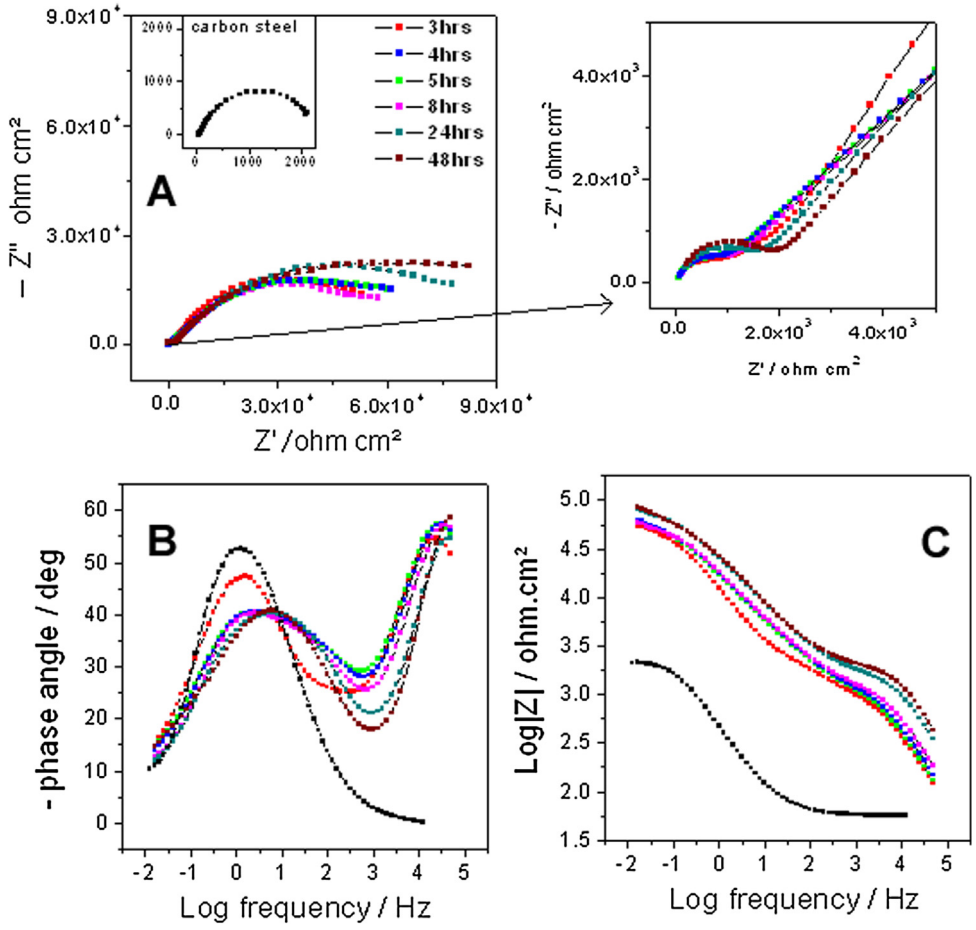


**Fig. 7 – Impedance diagrams. (A) Nyquist, (B) Bode $\theta$ × log $f$ and (C) Bode IZI × log $f$ for carbon steel treated with 400 ppm of octylsilanol hydrolyzed at pH 5.0 in the presence of 50 ppm Ce (III) for different immersion times.**

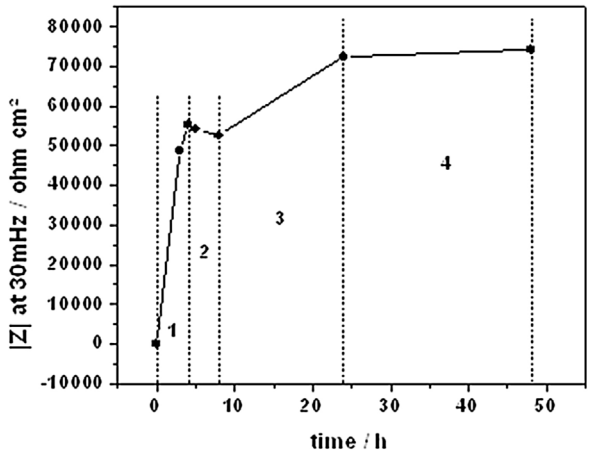


**Fig. 8 – Modulus of impedance at 30 mHz with increasing immersion time for carbon steel in the solution of octylsilanol hydrolyzed at pH 5.0 in the presence of 50 ppm Ce (III).**

$$Fe^{2+} + 2e \leftarrow Fe \quad (5)$$

$$O_2 + 2H_2O + 4e \rightarrow 4OH^- \quad (6)$$

$$Ce^{3+} + 3OH^- \rightarrow Ce(OH)_3 \quad (7)$$

Fig. 6a shows a schematic diagram of the inhibition mechanism with octylsilanol, where the coverage degree is low and the inhibition efficiency consequently is low. Fig. 6b also presents the inhibition mechanism with the mixture octylsilanol + Ce (III) ions, where the metallic surface is almost completely covered and the inhibition efficiency is very high.

### 3.9. *EIS with exposure time*

Assuming that the best condition obtained in this study was 400 ppm octylsilanol + 50 ppm Ce (III) ions, EIS measurements were performed along the immersion period to evaluate the evolution of the system. The impedance diagrams shown in Fig. 7 present this behavior. Capacitive arcs with increasing diameter represented in the Nyquist plots confirm a first step of the adsorption process where assembling of molecules occurs with time increasing the diameter of the capacitive arcs. Impedance modulus values, at low frequencies, in Bode plots, reveal the formation of an increasingly protective film on carbon steel, resulting in higher impedance modulus for longer immersion time. Bode plots for phase angle $\theta \times \log f$ show higher phase angle values for high frequencies and also for longer immersion times. There is a shift of this time constant for even higher frequencies, which indicates the presence of a protective film on the substrate. The time constant at low frequencies in the Bode plot $\theta \times \log f$, is due to a charge transfer phenomena occurring at the interface substrate/electrolyte, there is a slight shift of this time constant to higher values of frequency and also an enlargement of it, during the first hours of immersion. This behavior occurs due to increased resistance to charge transfer, which is due to the precipitation of cerium hydroxides in this region [24–26,39].

**Table 6 – Impedance modulus at 30 mHz for carbon steel treated with 400 ppm of octylsilanol hydrolyzed at pH 5.0 in the presence of 50 ppm Ce (III) for increasing immersion time.**

| Time (h) | \|Z\| at 30 mHz (Ω cm²) |
|---|---|
| 0 | 0 |
| 3 | 48,820 ± 600 |
| 4 | 55,195 ± 1769 |
| 5 | 54,171 ± 299 |
| 8 | 52,539 ± 1482 |
| 24 | 72,384 ± 981 |
| 48 | 74267 ± 1232 |

EIS measurements with immersion time in terms of impedance modulus, at 30 mHz, were determined for obtaining the kinetics of adsorption of the inhibitor molecule – octylsilanol – on the substrate and the protection provided by the Ce (III) ions through the hydroxides precipitates. The impedance modulus values at 30 mHz are summarized in Table 6. Fig. 8 shows the obtained kinetics curves of adsorption of the inhibitor molecule octylsilanol on carbon steel in 0.1 mol $L^{-1}$ NaCl. Generally, the self-assembly process of adsorbed molecules like long-chain alkane thiols can be described by two steps [16,23]. The first step consists in rapid adsorption of the molecule on the substrate, almost reaching its maximum

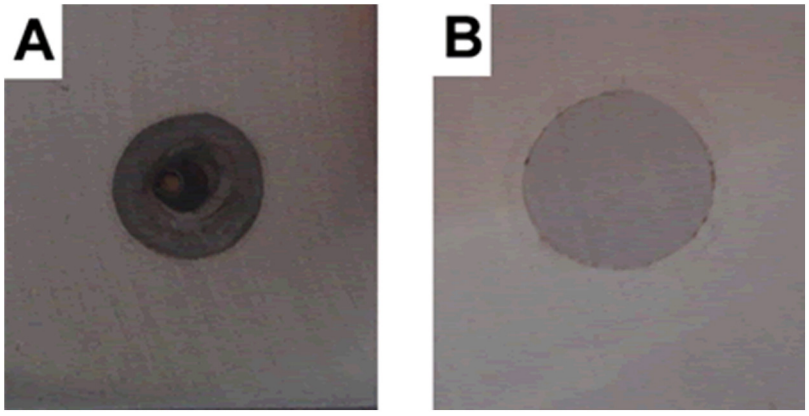


**Fig. 9 – Carbon steel samples after 48 h of immersion in (a) 0.1 mol $L^{-1}$ NaCl and (b) 0.1 mol $L^{-1}$ NaCl containing 400 ppm of octylsilanol + 50 ppm Ce(III).**

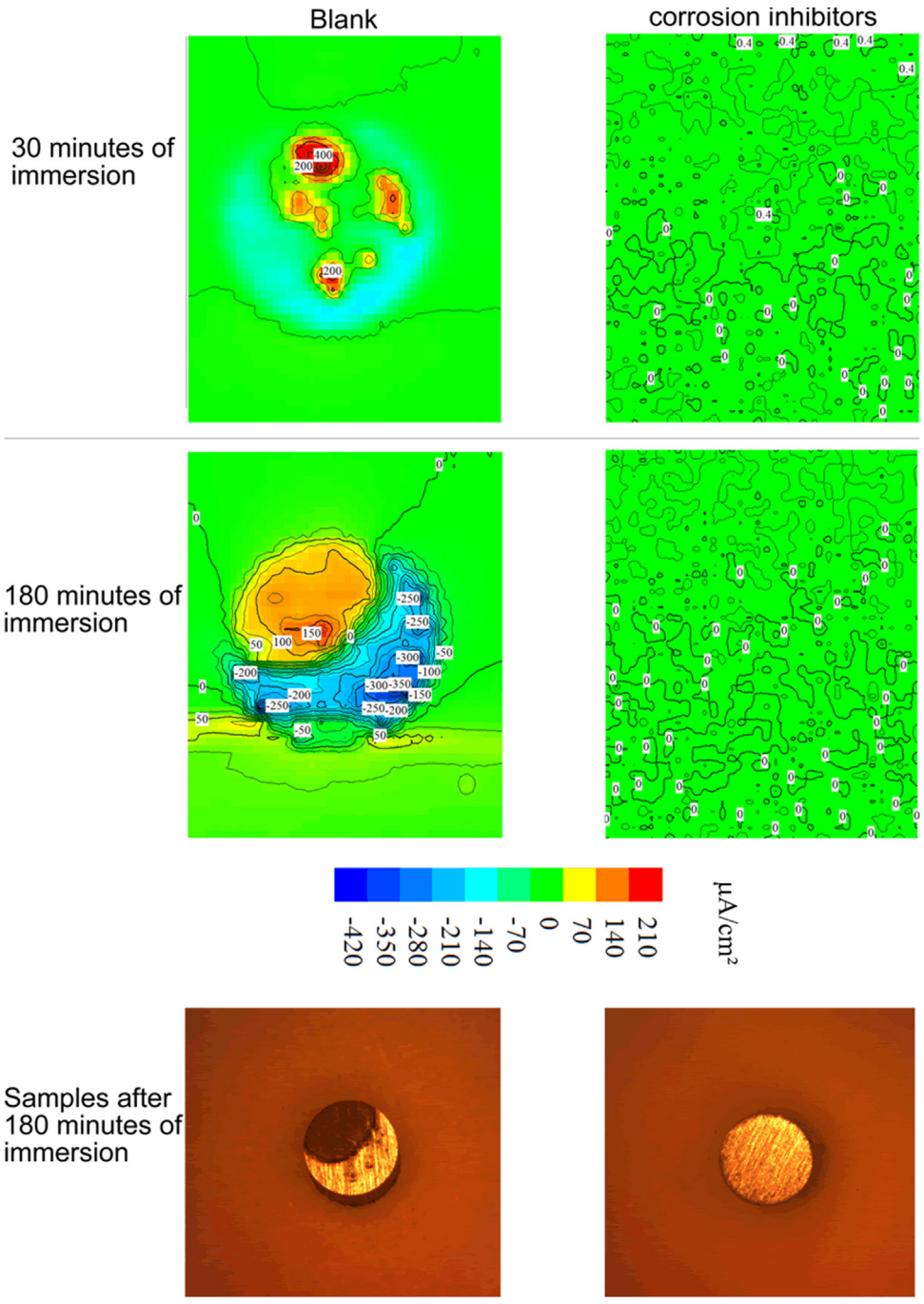


**Fig. 10 – SVET maps and samples aspect after 30 and 180 min of immersion in 0.01 mol $L^{-1}$ NaCl solution and 0.01 mol $L^{-1}$ NaCl solution containing 400 ppm of octylsilanol + 50 ppm Ce (III).**

level of coverage, about 80–90% of its final value, followed by a slower process of organization which takes about 10–20 h of immersion, leading long periods of time, until total coverage of the surface is reached [16,17]. In this second stage, it is usual to see the breakdown of the film formed, followed by a subsequent and quick build-up process ending with the final accommodation of the molecules on the substrate [16,40]. The octylsilanol molecule showed a similar behavior reported by some researchers for different silanes on aluminum and iron surfaces [23,24]. During the first hours of immersion (from 0 to 4 h), a rapid growth of the protective adsorbed silane layer on the substrate takes place while the precipitation of the Ce (III) ions occurs in the cathodic sites, which could be observed by the great increase in the impedance modulus (first stage in Fig. 8). Then, in stage 2 (from 4 to 8 h), the system showed a decrease in the protective effect, due the breakdown of the adsorbed film and, in the third stage (from 8 to 24 h), the re-adsorption and organization or self-assembly of the silanol molecules on the substrate surface takes place. From 24–48 h of immersion (fourth stage), no significant change is observed

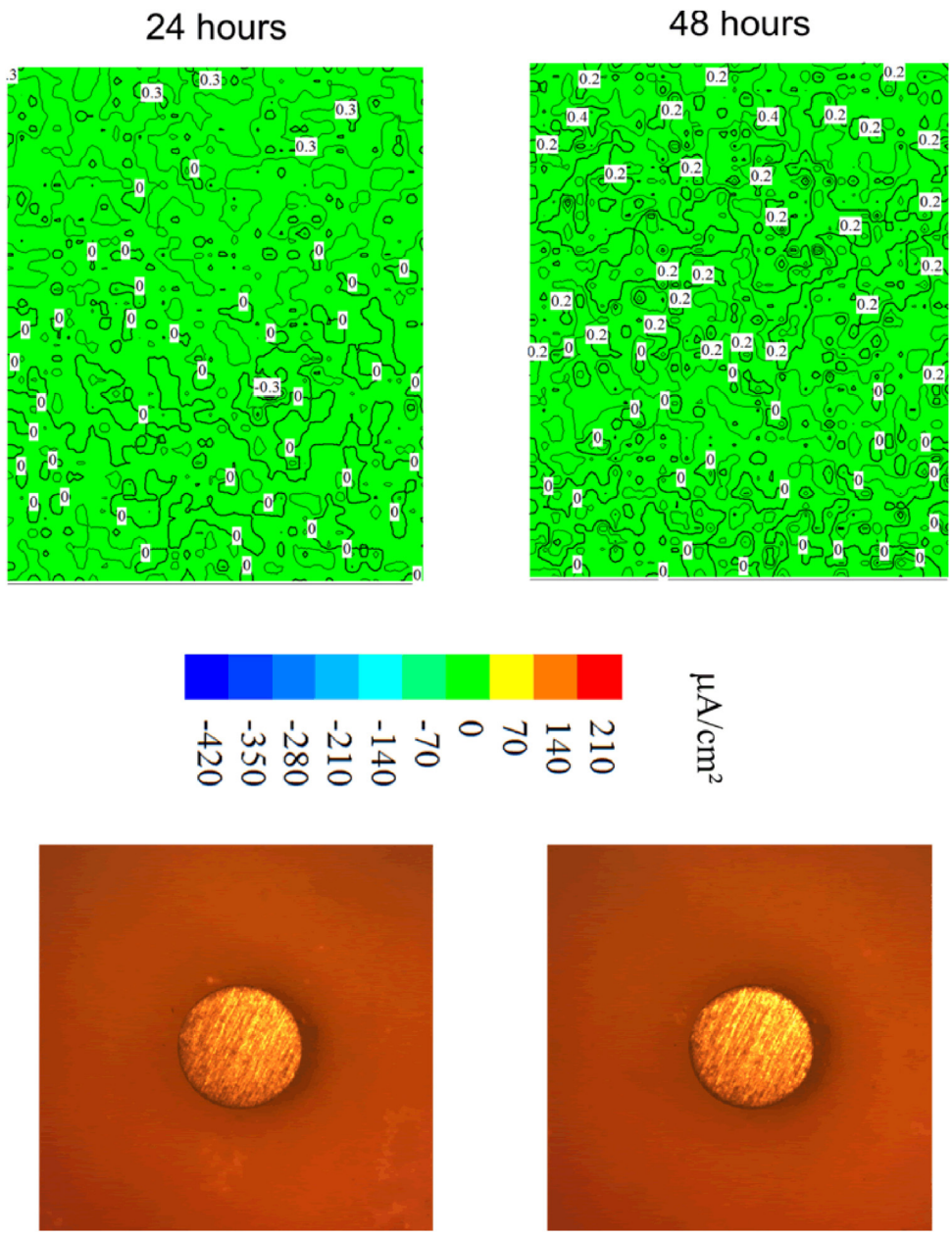


**Fig. 11 – SVET maps and samples aspect after 24 and 48 h of immersion in 0.01 mol $L^{-1}$ NaCl solution containing 400 ppm of octylsilanol + 50 ppm Ce (III).**

with a slight increase in the impedance modulus, characterizing the time necessary for the accommodation of the adsorbed molecules.

Fig. 9 shows the carbon steel surface after 48 h of immersion in NaCl 0.1 mol $L^{-1}$ electrolyte. Analyzing Fig. 8 one could observe that carbon steel surface remained protected after 48 h of immersion in the electrolyte containing corrosion inhibitors.

### 3.10. *Scanning vibrating electrode technique – SVET*

Fig. 10 shows the SVET maps of ionic currents above the substrate and its aspect in the presence of corrosion inhibitors – in the best combination defined by other techniques – and in the absence of corrosion inhibitors. These samples were evaluated after 30 min and 180 min ($E_{corr}$) of immersion in 0.01 mol $L^{-1}$ NaCl.

The SVET maps for the condition without corrosion inhibitors shows that the corrosion process started with intense anodic ionic currents, localized anodic zones and well-distributed cathodic zones in the edge of the substrate. After 180 min of immersion, the ionic currents are better distributed, with well-delimited zones. The high values of the ionic currents observed for this sample reveal the fast degradation of carbon steel in this electrolyte. The sample aspect after 180 min of immersion confirms the substrate degradation for this condition.

The SVET maps for the sample in the presence of corrosion inhibitors shows that the corrosion inhibitors rapidly promotes the substrate protection because there are no significant anodic and cathodic ionic currents in the map after 30 min of immersion. This behavior confirms that the corrosion inhibitors are capable of protecting the carbon steel surface against the oxidation process.

Fig. 11 presents the SVET maps and the substrate aspect for the samples with corrosion inhibitors, after 24 and 48 h of immersion in 0.01 mol $L^{-1}$ NaCl solution. From both SVET maps no significant ionic current density can be observed, which are in agreement with the results obtained by EIS for increasing immersion time, proving the permanence of the protective proprieties of the adsorbed silanol molecules and $Ce(OH)_3$ precipitates even for long immersion periods.

## 4. Conclusions

According to the results obtained, it was shown an excellent synergism between octylsilanol and Ce (III) ions as corrosion inhibitors which resulted in a % I.E. of about 96% in the best condition studied – 400 ppm octylsilanol + 50 ppm Ce (III) ions. This synergism was also demonstrated by polarization curves, where both anodic and cathodic branches of curves presented lower current densities due to octylsilanol adsorption in the anodic sites and precipitation of $Ce(OH)_3$ in the cathodic regions, protecting carbon steel from the aggressive environment. The contact angle measurements revealed a hydrophobic film formed on carbon steel by the actuation of the corrosion inhibitors.

The combination of 400 ppm octylsilanol + 50 ppm Ce (III) ions is more efficient and cheaper than reputable corrosion inhibitors for carbon steel in neutral solutions.

The Raman spectroscopy proved the octylsilanol adsorption and also cerium hydroxides precipitation on the carbon steel surface.

Even after 48 h of immersion, the corrosion inhibitors showed an excellent performance in the corrosion protection of carbon steel in NaCl 0.1 mol $L^{-1}$, due to persistence of the adsorbed film octylsilanol and by prolonged action of Ce (III) ions.

The SVET measurements were essential to show the fast and excellent corrosion inhibition provided by the corrosion inhibitors to carbon steel in chloride medium.

The SVET and EIS results with immersion time were very useful to determine and visualize the protective proprieties even for long exposure times in the electrolyte.

## Conflict of interests

The authors declare no conflicts of interest.

## Acknowledgements

The authors are thankful to Dr. Franklin Jaramillo from Universidad de Antioquia, Medellín, Colombia, for Raman spectroscopy measurements.

This work was supported by the Pró-Reitoria de Pesquisa da Universidade Federal de Minas Gerais (PRPq/UFMG) and by the Coordenação de Aperfeiçoamento de Pessoal de Nível Superior (CAPES).

## REFERENCES

[1] Verma C, Ebenso EE, Bahadur I, Quraishi MA. An overview on plant extracts as environmental sustainable and green corrosion inhibitors for metals and alloys in aggressive corrosive media. J Mol Liq 2018.
[2] Rani BEA, Basu BBJ. Green inhibitors for corrosion protection of metals and alloys: an overview. Int J Corros Scale Inhib 2012;2012:1–15.
[3] Zhang B, He C, Wang C, Sun P, Li F, Lin Y. Synergistic corrosion inhibition of environment-friendly inhibitors on the corrosion of carbon steel in soft water. Corros Sci 2015.
[4] Raja PB, Sethuraman MG. Natural products as corrosion inhibitor for metals in corrosive media – a review. Mater Lett 2008.
[5] Azzaoui K, Mejdoubi E, Jodeh S, Lamhamdi A, Rodriguez-Castellón E, et al. Eco friendly green inhibitor Gum Arabic (GA) for the corrosion control of mild steel in hydrochloric acid medium. Corros Sci 2017;129:70–81.
[6] Veys-Renaux D, Reguer S, Bellot-Gurlet L, Mirambet F, Rocca E. Conversion of steel by polyphenolic model molecules: corrosion inhibition mechanism by rutin, esculin, esculetol. Corros Sci 2018.
[7] Al-Sarawy AA, Fouda AS, El-Dein WAS. Some thiazole derivatives as corrosion inhibitors for carbon steel in acidic medium. Desalination 2008.
[8] Singh A, Ebenso EE, Quraishi MA. Corrosion inhibition of carbon steel in HCl solution by some plant extracts. Int J Corros Scale Inhib 2012.
[9] van Ooij WJ, Zhu D, Stacy M, Seth A, Mugada T, et al. Corrosion protection properties of organofunctional silanes – an overview. Tsinghua Sci Technol 2005.
[10] Zhu D, Van Ooij WJ. Corrosion protection of metals by water-based silane mixtures of bis-[trimethoxysilylpropyl]amine and vinyltriacetoxysilane. Prog Org Coat 2004.
[11] Van Schaftinghen T, Le Pen C, Terryn H, Hörzenberger F. Investigation of the barrier properties of silanes on cold rolled steel. Electrochim Acta 2004.
[12] Deflorian F, Rossi S, Fedrizzi L. Silane pre-treatments on copper and aluminium. Electrochim Acta 2006.
[13] Hansal WEG, Hansal S, Pölzler M, Kornherr A, Zifferer G, Nauer GE. Investigation of polysiloxane coatings as corrosion inhibitors of zinc surfaces. Surf Coatings Technol 2006.
[14] Frignani A, Zucchi F, Trabanelli G, Grassi V. Protective action towards aluminium corrosion by silanes with a long aliphatic chain. Corros Sci 2006.
[15] De Graeve I, Vereecken J, Franquet A, Van Schaftinghen T, et al. Silane coating of metal substrates: complementary use of electrochemical, optical and thermal analysis for the evaluation of film properties. Prog Org Coat 2007.
[16] Chico B, Galván JC, de la Fuente D, Morcillo M. Electrochemical impedance spectroscopy study of the effect of curing time on the early barrier properties of silane systems applied on steel substrates. Prog Org Coat 2007.
[17] Fedel M, Olivier M, Poelman M, Deflorian F, Rossi S, Druart ME. Corrosion protection properties of silane pre-treated powder coated galvanized steel. Prog Org Coat 2009.
[18] Subramanian V, Van Ooij WJ. Silane based metal pretreatments as alternatives to chromating. Surf Eng 1999.

[19] Capelossi VR, Aoki IV. Influence of sonication on anticorrosion properties of a sulfursilane film doped with Ce (IV) on galvannealed steel. Prog Org Coat 2013.
[20] Montemor MF, Cabral AM, Zheludkevich ML, Ferreira MGS. The corrosion resistance of hot dip galvanized steel pretreated with Bis-functional silanes modified with microsilica. Surf Coatings Technol 2006.
[21] Cotting F, Aoki IV. Smart protection provided by epoxy clear coating doped with polystyrene microcapsules containing silanol and Ce (III) ions as corrosion inhibitors. Surf Coatings Technol 2016;303.
[22] Forsyth M, Forsyth CM, Wilson K, Behrsing T, Deacon GB. ATR characterisation of synergistic corrosion inhibition of mild steel surfaces by cerium salicylate. Corros Sci 2002.
[23] Pepe A, Aparicio M, Durán A, Ceré S. Cerium hybrid silica coatings on stainless steel AISI 304 substrate. J Sol-Gel Sci Technol 2006.
[24] Yasakau KA, Zheludkevich ML, Lamaka SV, Ferreira MGS. Mechanism of corrosion inhibition of AA2024 by rare-earth compounds. J Phys Chem B 2006.
[25] Mardel J, Garcia SJ, Corrigan PA, Markley T, Hughes AE, Muster TH, et al. The characterisation and performance of Ce(dbp)3-inhibited epoxy coatings. Prog Org Coat 2011.
[26] Yasakau KA, Zheludkevich ML, Ferreira MGS. Lanthanide salts as corrosion inhibitors for AA5083. Mechanism and efficiency of corrosion inhibition. J Electrochem Soc 2008.
[27] Arenas MA, Conde A, De Damborenea JJ. Cerium: a suitable green corrosion inhibitor for tinplate. Corros Sci 2002.
[28] Ivušić F, Lahodny-Šarc O, Ćurković HO, Alar V. Synergistic inhibition of carbon steel corrosion in seawater by cerium chloride and sodium gluconate. Corros Sci 2015.
[29] Raja PB, Qureshi AK, Rahim AA, Awang K, Mukhtar MR, Osman H. Indole alkaloids of *Alstonia angustifolia* var. *latifolia* as green inhibitor for mild steel corrosion in 1 M HCl media. J Mater Eng Perform 2013.
[30] Humenyuk OL, Syza OI, Krasovs'Kyi OM. Inhibitor protection of steels in acid and neutral media by the derivatives of 2-mercaptobenzimidazole. Biomater Sci 2007.
[31] Bastos AC, Ferreira MG, Simões AM. Corrosion inhibition by chromate and phosphate extracts for iron substrates studied by EIS and SVET. Corros Sci 2006.
[32] Afshari V, Dehghanian C. Inhibitor effect of sodium benzoate on the corrosion behavior of nanocrystalline pure iron metal in near-neutral aqueous solutions. J Solid State Electrochem 2010.
[33] Bueno GV, Taqueda ME, De Melo HG, Guedes IC. Using a DOE and EIS to evaluate the synergistic effects of low toxicity inhibitors for mild steel. Brazil J Chem Eng 2015.
[34] Bahlakeh G, Ramezanzadeh M, Ramezanzadeh B. Experimental and theoretical studies of the synergistic inhibition effects between the plant leaves extract (PLE) and zinc salt (ZS) in corrosion control of carbon steel in chloride solution. J Mol Liq 2017.
[35] Koenig JL, Shih PTK. Raman studies of the glass fiber-silane-resin interface. J Colloid Interface Sci 1971.
[36] Johansson U, Holmgren A, Forsling W, Frost RL. Adsorption of silane coupling agents onto kaolinite surfaces. Clay Miner 1999.
[37] Scholes FH, Soste C, Hughes AE, Hardin SG, Curtis PR. The role of hydrogen peroxide in the deposition of cerium-based conversion coatings. Appl Surf Sci 2006.
[38] Griffiths PR. The handbook of infrared and Raman characteristic frequencies of organic molecules. Vib Spectrosc 1992.
[39] Cabral AM, Trabelsi W, Serra R, Montemor MF, Zheludkevich ML, Ferreira MGS. The corrosion resistance of hot dip galvanised steel and AA2024-T3 pre-treated with bis-[triethoxysilylpropyl] tetrasulfide solutions doped with $Ce(NO_3)_3$. Corros Sci 2006.
[40] Montemor MF, Pinto R, Ferreira MGS. Chemical composition and corrosion protection of silane films modified with $CeO_2$ nanoparticles. Electrochim Acta 2009;54:5179–89.